# Energetics of Midvelocity Emissions in Peripheral Heavy Ion Collisions at Fermi Energies

A. Mangiarotti, P. R. Maurenzig, A. Olmi, S. Piantelli, L. Bardelli, A. Bartoli, M. Bini, G. Casini, C. Coppi, A. Gobbi,* G. Pasquali, G. Poggi, A. A. Stefanini, N. Taccetti, and E. Vanzi

*Sezione INFN and Università di Firenze, Via G. Sansone 1, I-50019 Sesto Fiorentino, Italy*

(Received 28 May 2004; published 30 November 2004)

Peripheral and semiperipheral collisions have been studied in the system $^{93}$Nb + $^{93}$Nb at 38*A* MeV. The evaporative and midvelocity components of the light charged particle and intermediate mass fragment emissions have been carefully disentangled. In this way it was possible to obtain the average amount not only of charge and mass, but also of energy, pertaining to the midvelocity emission, as a function of an impact parameter estimator. This emission has a very important role in the overall balance of the reaction, as it accounts for a large fraction of the emitted mass and for more than half of the dissipated energy. As such, it may give precious clues on the microscopic mechanism of energy transport from the interaction zone toward the target and projectile remnants.

DOI: 10.1103/PhysRevLett.93.232701 PACS numbers: 25.70.Lm, 25.70.Pq

In peripheral to midcentral collisions of heavy ions at *Fermi energies* [$E_{\mathrm{beam}} = (30–50)A$ MeV] an intense emission of light charged particles (LCPs) and especially of intermediate mass fragments (IMFs) at velocities between those of the projectilelike and targetlike fragments (PLFs and TLFs) is observed [1–9]. These so-called "neck emissions" or "midvelocity emissions" may be seen as an intermediate stage between the fast three-body processes found at lower energies [10,11] and the explosion of the "participant zone" at much higher energies.

At low beam energies ($\lesssim 15A$ MeV), the exchange of nucleons between PLF and TLF, whose mean fields merge for a prolonged time, plays a dominant role in the energy dissipation process, but it is very difficult to have experimental access to probes directly connected to the mechanism of matter exchange. At high energies ($\gtrsim 100A$ MeV), because of the small de Broglie wavelength of the nucleons and the reduced Pauli blocking, the energy dissipation mechanism is dominated by direct nucleon-nucleon collisions in the overlap between projectile and target, and the short interaction time does not allow a significant heat transport to the nonoverlapping zones. At Fermi energies the energy dissipation is already significantly localized in the midvelocity region—as quantitatively demonstrated in this Letter—while the interaction time may still be long enough to allow the transfer of a sizable amount of energy to the surrounding nuclear matter, thus resulting in an excited PLF and TLF (henceforth indicated with PLF* and TLF*).

To clarify the mechanism leading to midvelocity emissions, an important aspect is represented by the amount of energy involved in these emissions [12], as compared with the excitation energy left in the PLF* or TLF*. This may yield clues about the transition between the low-energy dissipative collisions (where the energy removed from the relative motion is totally converted into excitation of PLF* and TLF*) and the high-energy participant-spectator regime. We present here, for the first time, a direct simultaneous determination of the energy involved in the midvelocity and in the evaporative emissions.

The results of this Letter refer to the collision $^{93}$Nb + $^{93}$Nb at 38*A* MeV, as a part of a systematic study [13–16] of heavy ion collisions performed at the Superconducting Cyclotron of the Laboratori Nazionali del Sud of INFN in Catania, with the FIASCO setup [17]. The apparatus consists of gas detectors (measuring heavy products with $E \gtrsim 0.1A$ MeV in $\approx 70\%$ of the forward hemisphere), $\Delta E$-$E$ silicon telescopes (determining charge and mass of PLFs below the grazing angle), and phoswich telescopes (for isotopic identification of LCPs and elemental identification of IMFs with $Z \geq 3$, in about 30% of the forward hemisphere).

This Letter is focused on two-body events, by far prevailing in (semi-)peripheral collisions, where two and only two large reaction remnants are detected by the gas counters (which are fully efficient for heavy fragments with $Z \gtrsim 10$–$14$). This allows one to have as clean as possible kinematics, profiting in the best way of FIASCO's ability to detect also the TLF, with the aim of studying the energy associated to midvelocity emissions in a situation where their release represents the dominant process.

The setup measures the secondary quantities of PLF and TLF after the sequential evaporation, while primary quantities of the excited PLF* and TLF* are estimated from the measured velocities with the kinematic coincidence technique [18]. As an indicator of the centrality of the collision we have chosen a kinematic variable, defined as $\mathrm{TKEL} = E_{\mathrm{in}}^{\mathrm{c.m.}} - \frac{1}{2}\tilde{\mu}v_{\mathrm{rel}}^2$, where $E_{\mathrm{in}}^{\mathrm{c.m.}}$ is the center-of-mass (c.m.) energy in the entrance channel, $\tilde{\mu}$ is the reduced mass calculated with the masses of the kinematic reconstruction (forced to add up to the total mass of the system and thus overestimated), and $v_{\mathrm{rel}}^2$ is the reconstructed primary relative velocity between PLF* and TLF*. While at low incident energies (where reactions are strictly binary), TKEL truly represents the total kinetic energy loss of the collision, it is important to

 

emphasize that in this work, where a sizable midvelocity emission is present, TKEL is used just as an order parameter for classifying the events in bins of different impact parameter. Indeed, the kinematic analysis of events generated by a quantum molecular dynamics (QMD) code [19] shows a strict correlation between TKEL and impact parameter [13].

The average multiplicities of charged particles, $\langle \mathcal{M}_{C_i} \rangle$ (henceforth we use the brackets $\langle\,\rangle$ to indicate averages over events in a given bin of TKEL), were obtained from the distributions of the experimental yields of $p$, $d$, $t$, He, and IMFs in the $(v_\perp, v_\parallel)$ plane, after correcting for the finite geometrical coverage of the phoswiches. Here $v_\parallel$ and $v_\perp$ are the velocity components parallel and perpendicular, respectively, to the asymptotic PLF*-TLF* separation axis in the c.m. system; for the TKEL range addressed in this work, the c.m. separation axis lies within about 10° from the beam axis. The advantage of using a symmetric collision is that the forward-going particles (those with $v_\parallel \geq 0$) must have the same average characteristics as the backward-going ones. Therefore, in this Letter all multiplicities refer only to forward-emitted particles, for which the setup has a much better solid angle coverage and threshold effects do not play any role (all particles having laboratory energies larger than $\approx 9.5A$ MeV). In a symmetric system, adding up the charges of forward-emitted LCPs and IMFs to the charge of the PLF should reproduce, on average, the projectile charge. The deficit of about half a charge unit shown in Fig. 1 was corrected by slightly rescaling the contribution of all charged reaction products in each TKEL bin.

Another advantage of a symmetric collision is that the contribution of the free neutrons (unmeasured) can be estimated from mass conservation. In fact, the average multiplicity of all the undetected forward-emitted free neutrons is given by $\langle \mathcal{M}_n \rangle = A_{\rm proj} - \sum_i A_{C_i} \langle \mathcal{M}_{C_i} \rangle - \langle A_{\rm sec} \rangle$, where $\langle A_{\rm sec} \rangle$ is the average secondary mass of the PLF (measured with the silicon telescopes) and $A_{C_i}$ are the mass numbers of the different charged particle species. In doing so, the common assumption $A = 2Z$ was used for estimating the masses of the IMFs, which were not isotopically resolved; we verified that, as the IMF multiplicities are small ($\lesssim 1$), the uncertainty caused by this assumption is less than one mass unit. Great care was also devoted to determining $A_{\rm sec}$ via time-of-flight measurements with both gas and silicon detectors: the obtained secondary masses were always in good agreement with the so-called evaporation attractor line (EAL) [20], except for low TKEL where the excitation is low and the mass of the PLF* is close to the stability valley (which is slightly more neutron rich than the EAL).

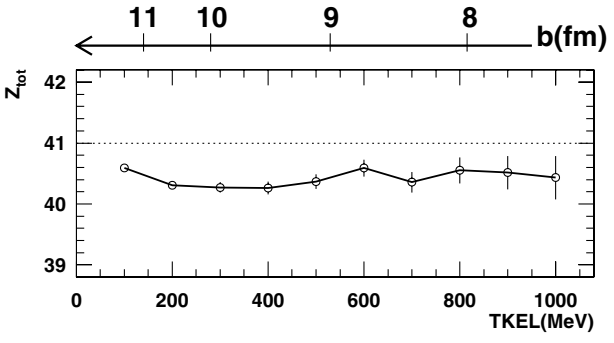


FIG. 1. Average total charge of forward-going products. The dotted line indicates the charge of a Nb projectile, while the arrow on top shows the impact parameter scale estimated from QMD calculations [19].

It is relatively simple to perform a check of the energy balance of all forward-going reaction products. In fact, the total energy is obtained (for each bin of TKEL) by adding the c.m. kinetic energy of the PLF residue to the energy associated to the emission of all forward-going particles, without distinction of their production mechanism, namely,

$$\langle E^{\rm c.m.}_{\rm forw} \rangle = \sum_i \overline{k}^{\rm c.m.}_{C_i} \langle \mathcal{M}_{C_i} \rangle + \overline{k}^{\rm c.m.}_n \langle \mathcal{M}_n \rangle - Q_{\rm tot}, \qquad (1)$$

where $\overline{k}^{\rm c.m.}_{C_i}$ is the average (efficiency corrected) c.m. kinetic energy of the charged particles of the $i$th species and the sum extends over the different species; $\overline{k}^{\rm c.m.}_n$ is the average c.m. kinetic energy of the free neutrons (estimated from the protons after correcting for the lack of Coulomb repulsion); $Q_{\rm tot}$ is the $Q$ value for disassembling the projectile into the average secondary PLF, plus as many neutrons, LCPs, and IMFs as given by their respective multiplicities. We expect to come close to the c.m. kinetic energy of the incoming projectile (about 885 MeV), having disregarded only the energy of $\gamma$ rays, which are mainly emitted at the end of the evaporation chain. Indeed the sum falls short of the projectile energy by less than 15 MeV at small TKEL values (rising to about 50 MeV at TKEL $\approx$ 500 MeV), thus providing confidence in the results of the present analysis.

It is much more difficult to separate the energy associated to the midvelocity emissions from that associated with the sequential evaporation from the fully equilibrated PLF*. First, it is necessary to estimate the yields of the two components. In peripheral collisions, this is feasible because the PLF can always be safely distinguished from the TLF (on the basis of the phase-space distributions of the heavy remnants) and the most forward part of the LCP and IMF emission can be ascribed to a pure evaporative process. These same considerations advise against extending the study to more central collisions (that is, in the present work, beyond TKEL $\approx$ 600 MeV). The procedure is based on the distributions of the emission angle $\theta$ in the PLF frame [see, e.g., Fig. 2(a)], taking the PLF*-TLF* separation axis as polar axis. For pure evaporation and neglecting recoil effects (which are important only at small TKEL), one expects approximately a $\sin(\theta)$ distribution for a source with zero

spin and a somewhat flatter shape for nonzero spin [see, e.g., Fig. 2(b)]. In reality, normalizing the distributions below 30°, one finds that for all particle species the data have a large excess at backward angles (with a tail extending well below $\theta = 90°$), which is ascribed to midvelocity emissions. Therefore the evaporative multiplicities were extrapolated from the experimental data measured, conservatively, in the range $0° \leq \theta \leq 30°$ (but the results do not change appreciably when extending the upper limit up to 45°), while the spin of the PLF* was deduced from the out-of-plane angular distributions [15]. The multiplicities associated with the midvelocity emissions were then determined from the difference between the total multiplicities and the evaporative ones.

It is now necessary to also make a hypothesis on the subdivision of $\langle \mathcal{M}_n \rangle$ between the midvelocity emission, $\langle \mathcal{M}_n^{\mathrm{midv}} \rangle$, and the subsequent statistical evaporation of the PLF*, $\langle \mathcal{M}_n^{\mathrm{evap}} \rangle$. Following the findings of Ref. [21] we have assumed, as a working hypothesis, that the overall neck emissions (and consequently also the primary PLF*) have the same $N/Z$ ratio (= 1.27) as the entire system. However, it will be shown that other hypotheses on the $N/Z$ ratio at midvelocity do not change appreciably the results of this Letter.

Finally, one needs, for the various particle species, the average kinetic energies of the evaporative component. Since, in the emitting system, the kinetic energies of evaporated particles do not depend on emission angle, the values obtained in the forward 30° range (in the PLF* frame) are used for the whole evaporative emission.

It is now possible to estimate the total mass evaporated from the excited PLF* and the associated energy (measuring the initial excitation energy) by summing up masses and kinetic energies (the superscript "PLF" reminds us that they are not in the c.m. frame) of neutrons, LCPs, and IMFs weighted with their evaporative multiplicities:

$$\langle A_{\mathrm{evap}} \rangle = \sum_i A_{C_i} \langle \mathcal{M}_{C_i}^{\mathrm{evap}} \rangle + \langle \mathcal{M}_n^{\mathrm{evap}} \rangle, \tag{2}$$

$$\langle E_{\mathrm{evap}} \rangle = \sum_i \overline{k}_{C_i,\mathrm{evap}}^{\mathrm{PLF}} \langle \mathcal{M}_{C_i}^{\mathrm{evap}} \rangle + \overline{k}_{n,\mathrm{evap}}^{\mathrm{PLF}} \langle \mathcal{M}_n^{\mathrm{evap}} \rangle - Q_{\mathrm{evap}}, \tag{3}$$

where $\overline{k}_{C_i,\mathrm{evap}}^{\mathrm{PLF}}$ is the average (efficiency corrected) kinetic energy of the evaporated charged particles of the $i$th species (in the PLF frame, evaluated for $\theta \leq 30°$); $\overline{k}_{n,\mathrm{evap}}^{\mathrm{PLF}}$ is the average kinetic energy of the evaporated neutrons (estimated from that of the protons minus an average Coulomb barrier); $Q_{\mathrm{evap}}$ is the $Q$ value for disassembling the average primary PLF* into the average secondary PLF, plus as many neutrons, LCPs, and IMFs as given by their respective evaporative multiplicities. The obtained results are shown in Figs. 3(a) and 3(c). Here, as in the other panels, the symbols correspond to the adopted value of 1.27 for the $N/Z$ of the total midvelocity emissions, while the dashed and dotted lines refer to the rather $n$-poor and $n$-rich values of 1.10 and 1.44, respectively, which produce a variation of roughly ±50% in $\langle \mathcal{M}_n^{\mathrm{midv}} \rangle$. As anticipated, such a large variation of $N/Z$ has a limited effect on the presented results. The behavior of both $\langle A_{\mathrm{evap}} \rangle$ and $\langle E_{\mathrm{evap}} \rangle$ is very regular, displaying a steady, almost linear increase with increasing TKEL. This suggests that TKEL, even in the presence of a sizable midvelocity emission, remains nevertheless a good indicator of the average excitation energy of the PLF* (and of the TLF* as well) [15]. The obtained average energetic cost per evaporated nucleon is about 9–10 MeV, in reasonable agreement with results of the statistical code GEMINI [22].

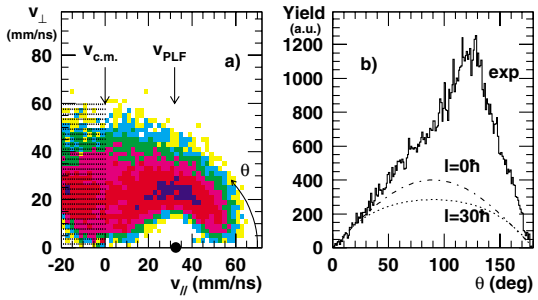


FIG. 2 (color online). (a) Experimental yield of $\alpha$ particles, at TKEL ≈ 600 MeV, in the $(v_\perp, v_\parallel)$ plane with respect to the PLF*-TLF* separation axis; the dot at $v_\parallel \approx 32$ mm/ns is the location of the PLF* source. (b) Corresponding angular distribution in the PLF frame (histogram) and results of simulations for an evaporating source with spin $0\hbar$ and $30\hbar$ (dashed and dotted lines, respectively, normalized in the range $0° \leq \theta \leq 30°$).

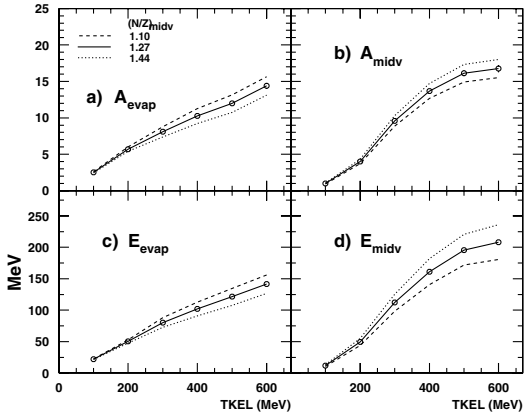


FIG. 3. Average total mass of (a) the PLF* evaporation, $\langle A_{\mathrm{evap}} \rangle$, and (b) the forward-going midvelocity emissions, $\langle A_{\mathrm{midv}} \rangle$; average amount of energy involved in (c) the PLF* evaporation, $\langle E_{\mathrm{evap}} \rangle$, and (d) the forward-going midvelocity emissions, $\langle E_{\mathrm{midv}} \rangle$. The data are presented as a function of TKEL and the different curves correspond to different $N/Z$ values for the midvelocity emissions.

Subtracting from the mass and energy of all emitted particles the contribution of the evaporation, one can estimate the part pertaining to the midvelocity emissions

$$\langle A_{\mathrm{midv}}\rangle = \left(\sum_i A_{C_i}\langle \mathcal{M}_{C_i}\rangle + \langle \mathcal{M}_n\rangle\right) - \langle A_{\mathrm{evap}}\rangle, \quad (4)$$

$$\langle E_{\mathrm{midv}}\rangle = \langle E^{\mathrm{c.m.}}_{\mathrm{forw}}\rangle - (\langle E_{\mathrm{evap}}\rangle + \langle K_{\mathrm{transl}}\rangle). \quad (5)$$

As the kinetic energies of $\langle E^{\mathrm{c.m.}}_{\mathrm{forw}}\rangle$ are evaluated in the c.m. reference frame and those of $\langle E_{\mathrm{evap}}\rangle$ in the PLF frame, the translational kinetic energy of the whole pattern of evaporated particles (due to the motion of the source) was taken into account with the term $\langle K_{\mathrm{transl}}\rangle \approx \frac{1}{2} m_N \langle A_{\mathrm{evap}}\rangle \langle v^2\rangle$, where $m_N$ is the nucleon mass, $A_{\mathrm{evap}}$ is the mass number of the total evaporation from PLF*, and $v$ is the c.m. velocity of the PLF residue [23].

The results of Eqs. (4) and (5) are shown in Figs. 3(b) and 3(d), respectively. With increasing TKEL, both $\langle A_{\mathrm{midv}}\rangle$ and $\langle E_{\mathrm{midv}}\rangle$ first increase almost linearly and then flatten (at values around 17 and 200 MeV, respectively). The origin of this flattening, which is present also in the partial contributions of all LCPs and IMFs, is still an open question and will be the subject of further investigation [24]. The comparison of Figs. 3(c) and 3(d) shows that, at a given TKEL, up to about half of the energy goes into the midvelocity component, which is really an essential aspect of the reaction and may represent [25] the prodrome of the multifragmentation of the whole system, occurring in central collisions.

In short, it can be stated that $\langle E_{\mathrm{midv}}\rangle$ and $\langle E_{\mathrm{evap}}\rangle$ are comparable and this statement holds in spite of several systematic uncertainties that affect their evaluation (conservatively, altogether up to 30% of the quoted values). So in the Fermi domain, an important part of the dissipated energy, initially stored in the translational motion of the projectile, is localized in the new midvelocity emission. This mechanism has an important role in the overall balance of the reaction, both in terms of the emitted mass (charge) and energy [26]. The emission pattern of midvelocity reaction products in the $(v_\perp, v_\parallel)$ plane (obtained by subtraction of the evaporative component) is qualitatively similar to that shown in Ref. [14].

Finally, since the amount of dissipated energy localized in the midvelocity matter is comparable to that in the PLF* or TLF*, and the mass of the emitting zone (two sources as schematized in Ref. [14] or, more realistically, a whole distribution of sources) is certainly smaller, one may expect for the midvelocity matter a value of $E^*/A$ (of the order of 7–13 MeV, depending on the assumed source size) significantly larger than that of the evaporative source ( $\lesssim 2$ MeV for the data of this work). It is well known experimentally that with increasing $E^*/A$ the disassembly properties of nuclear matter radically change, leading to a preferential formation of IMFs [27,28]. A large $E^*/A$ value is therefore consistent with the observation of a preferential emission of IMFs at midvelocity. Experimental data on the deposition of energy in the midvelocity matter may represent an important benchmark for the most sophisticated microscopic calculations [29–32]. When such comparisons with the data become available, one may hope to gain some new insight on the mechanism at the basis of the large, strongly localized, energy deposition as well as on the transport of internal energy from the interaction zone to the cold projectile and target remnants.

Many thanks are due the staff of LNS for continuous support and for providing very good pulsed beams.

*Present address: Vicolo dei Conti 6, CH-6932 Breganzona, Switzerland.

[1] C. P. Montoya *et al.*, Phys. Rev. Lett. **73**, 3070 (1994).
[2] J. Tõke *et al.*, Phys. Rev. Lett. **75**, 2920 (1995).
[3] J. F. Dempsey *et al.*, Phys. Rev. C **54**, 1710 (1996).
[4] J. Lukasik *et al.*, Phys. Rev. C **55**, 1906 (1997).
[5] E. Plagnol *et al.*, Phys. Rev. C **61**, 014606 (1999).
[6] P. M. Milazzo *et al.*, Phys. Lett. B **509**, 204 (2001).
[7] B. Davin *et al.*, Phys. Rev. C **65**, 064614 (2002).
[8] J. Colin *et al.*, Phys. Rev. C **67**, 064603 (2003).
[9] A. Pagano *et al.*, Nucl. Phys. **A734**, 504 (2004).
[10] P. Glässel *et al.*, Z. Phys. A **310**, 189 (1983).
[11] G. Casini *et al.*, Phys. Rev. Lett. **71**, 2567 (1993).
[12] Y. Larochelle *et al.*, Phys. Rev. C **59**, R565 (1999).
[13] S. Piantelli, Ph.D. thesis, Florence University, 2001.
[14] S. Piantelli *et al.*, Phys. Rev. Lett. **88**, 052701 (2002).
[15] A. Mangiarotti, Ph.D. thesis, Florence University, 2003.
[16] S. Piantelli *et al.* (to be published).
[17] M. Bini *et al.*, Nucl. Instrum. Methods Phys. Res., Sect. A **515**, 497 (2003).
[18] G. Casini *et al.*, Nucl. Instrum. Methods Phys. Res., Sect. A **277**, 445 (1989).
[19] J. Lukasik and Z. Majka, Acta Phys. Pol. B **24**, 1959 (1993).
[20] R. J. Charity, Phys. Rev. C **58**, 1073 (1998).
[21] L. G. Sobotka *et al.*, Phys. Rev. C **62**, 031603R (2000).
[22] R. J. Charity *et al.*, Nucl. Phys. **A483**, 371 (1988).
[23] This neglects corrections ($\lesssim 10$ MeV) due to correlations of $A_{\mathrm{evap}}$ with $v^2$; the correct expression $\langle K_{\mathrm{transl}}\rangle = \frac{1}{2} m_N \langle A_{\mathrm{evap}} v^2\rangle$ is actually unusable even with $4\pi$ detectors, as it requires one to identify the origin of each particle.
[24] The flattening of $\langle A_{\mathrm{midv}}\rangle$ may be partly induced by the selection of binary events: events with a more massive interaction zone are likely to emit larger fragments and have a larger chance of being classified as three-body events.
[25] V. Baran, M. Colonna, and M. Di Toro, Nucl. Phys. **A730**, 329 (2004).
[26] A. Gobbi *et al.* (to be published).
[27] C. A. Ogilvie *et al.*, Phys. Rev. Lett. **67**, 1214 (1991).
[28] L. Beaulieu *et al.*, Phys. Rev. C **54**, R973 (1996).
[29] H. Feldmeier, Nucl. Phys. **A515**, 147 (1990).
[30] A. Ono *et al.*, Prog. Theor. Phys. **87**, 1185 (1992).
[31] A. Ono, Phys. Rev. C **59**, 853 (1999).
[32] H. Feldmeier and J. Schnack, Rev. Mod. Phys. **72**, 655 (2000).